DALTON
FULL PAPER

# A study on the heterodinuclear cryptates [LnCuL(DMF)](ClO$_4$)$_2$·MeCN (Ln = Gd, Eu, Tb, Dy, Y) — synthesis, characterization, magnetic and electrochemical properties

**Qiu-Yun Chen,[a,c] Qin-Hui Luo,*[a,c] De-Gang Fu[a] and Jiu-Tong Chen[b]**

[a] *State Key Laboratory of Coordination Chemistry, Coordination Chemistry Institute, Nanjing University, Nanjing 210093, P. R. China*
[b] *Fuzhou State Key Laboratory of Structure Chemistry, Fuzhou 350002, P. R. China*
[c] *State Key Laboratory of Lanthanide Material Chemistry, Beijing University, Beijing, 100008, P. R. China*

***Received 25th February 2002, Accepted 2nd May 2002***
***First published as an Advance Article on the web 6th June 2002***

Five heterodinuclear cryptates [LnCuL(DMF)](ClO$_4$)$_2$·MeCN (Ln = Gd, Eu, Tb, Dy, Y) were synthesized (L represents the deprotonated anionic cryptand obtained by condensation of tris(2-aminoethyl)amine with 2,6-diformyl-4-chlorophenol). The ES-MS spectra of five cryptates showed that the Ln(III)–Cu(II) cores are very stable in solution. The crystal structure of [EuCuL(DMF)](ClO$_4$)$_2$ was determined and was compared with those of mono- and hetero-nuclear copper(II) with the same ligand. The Gd(III)–Cu(II) cryptate displayed weaker intramolecular ferromagnetic interactions than the complexes with two phenolate bridges. The $E_{1/2}$ values of Cu(II)/Cu(I) were influenced by Ln(III) in the cryptates and shifted negatively comparing with free $Cu^{2+}$. The degree of negative-shift is in the order: Dy > Tb > Gd > Eu.

## Introduction

Due to their unique properties compared to analogous mononuclear and homodinuclear complexes there has been a great deal of recent interest in heterodinuclear complexes.[1] These properties are involved in mimicking the active centers of some metalloenzymes,[2] in the design of new materials[3] and in the preparation of catalysts or as the precursors of catalysts.[4] The mononuclear lanthanide complexes are utilized as luminescent probes,[5] NMR shift agents and as magnetic resonance imaging agents,[6] *etc*.[7] Despite this, heterodinuclear complexes containing both transition metal and lanthanide ions are still rarely reported[8] and studies on these complexes are mostly concentrated on magnetic properties of the acyclic complexes.[9] The cryptates have good thermodynamic stability and kinetic inertness toward metal dissociation. Lehn, Sabbatini and co-workers presented pioneering studies on lanthanide polyaza-cryptates containing three 2,2′-bipyridine units and their pyridine *N*-oxide units.[10] Since 1997 iminophenolate (Robson-type) cryptates have been investigated intensively.[11] Phenol-based mononuclear and homodinuclear lanthanide cryptates have been obtained by Nelson[12] and Fenton,[13] respectively. Recently, a'Robson-type' d–f heterodinuclear cryptate was synthesized by us,[14a] and its magnetic interaction was also reported.[14b] In order to understand the properties of the d–f heterodinuclear cryptates and their d–f interaction, we successfully synthesized five new heterodinuclear cryptates [LnCuL(DMF)](ClO$_4$)$_2$·MeCN [Ln = Gd, Eu, Tb, Dy, Y, L denotes the deprotonated anionic cryptand synthesized by condensation of tris(2-aminoethyl)amine (tren) with 2,6-diformyl-4-chlorophenol (dcp)] (Scheme 1). The ES-MS spectra of five cryptates showed that each was a strict heterodinuclear entity and very stable in solution, beneficial for the study of their electrochemical properties. The structural regularities of heterodinuclear cryptates were found by comparison of crystal structure data with those of some mononuclear and heterodinuclear cryptates. Their electrochemical and magnetic properties arising from the interaction between d–f metal ions were also investigated.

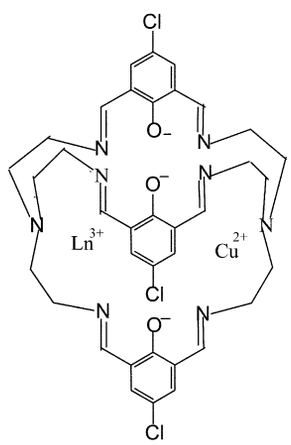


**Scheme 1** The structure formulae of complex cations used in this study (Ln = Gd, **1**; Eu, **2**; Tb, **3**; Y, **4**; Dy, **5**).

## Experimental

### Synthesis and characterization

Ln(NO$_3$)$_3$·6H$_2$O were prepared by dissolving Ln$_2$O$_3$ (99.99%) in an excess of nitric acid; 2,6-diformyl-4-chlorophenol (dcp)[15] and tris(2-aminoethyl)amine (tren)[16] were prepared by literature methods. Their physical constants and spectral data are in agreement with literature values. All starting materials were of reagent grade; the solvents were purified by general methods.

**[GdCuL(DMF)](ClO$_4$)$_2$·MeCN 1.** Mononuclear gadolinium(III) cryptate (0.117 g, 0.1 mmol), synthesized by the previously reported method,[23] was dissolved in methanol (15 cm$^3$) containing a small amount of DMF (1.0 cm$^3$). After the pH of the solution was adjusted to 7–8 with an excess of CaH$_2$, and filtered, hydrated copper perchlorate (0.037 g, 0.1 mmol) was added to the filtrate and the mixture refluxed for *ca.* 4 h. The solution was then concentrated until a red product formed.

DOI: 10.1039/b201970a

Yield: 0.0820 g, 65%. Found: C, 38.64; H, 3.75; N, 10.56; $C_{41}H_{46}Cl_5N_{10}O_{12}CuGd$ requires: C, 38.30; H, 3.65; N, 11.04%. IR (KBr, $cm^{-1}$) 1645s [$\nu$(C=N)]; 1541s [$\nu$(C–O)]; 1090s [$\nu(ClO_4)$]; 625m [$\nu(ClO_4)$]. [UV-Vis($\lambda_{max}$(nm), MeCN)]: 851 (53 $mol^{-1}$ $dm^3$ $cm^{-1}$), 495(shoulder), 378 (17400 $mol^{-1}$ $dm^3$ $cm^{-1}$), 244 (64200 $mol^{-1}$ $dm^3$ $cm^{-1}$), 227 (73300 $mol^{-1}$ $dm^3$ $cm^{-1}$). $\Lambda_m$ (DMF, 298 K): 142 S $cm^2$ $mol^{-1}$. The complex can be dissolved in DMF and DMSO and it has low solubility in MeCN and MeOH.

**[EuCuL(DMF)](ClO$_4$)$_2$·MeCN 2.** Was synthesized by a method similar to that for **1** described above. Yield: 0.057 g, 45%. Found; C, 38.90; H, 3.70; N, 10.72; $C_{41}H_{46}Cl_5N_{10}O_{12}CuEu$ requires: C, 38.97; H, 3.67; N, 11.08%. IR (KBr, $cm^{-1}$): 1645s [$\nu$(C=N)]; 1541s [$\nu$(C–O)]; 1092s [$\nu(ClO_4)$]; 625m [$\nu(ClO_4)$]. [UV-Vis($\lambda_{max}$(nm), MeCN)]: 852 (60 $mol^{-1}$ $dm^3$ $cm^{-1}$), 495(shoulder), 377 (19100 $mol^{-1}$ $dm^3$ $cm^{-1}$) 244 (72800 $mol^{-1}$ $dm^3$ $cm^{-1}$), 227 (83100 $mol^{-1}$ $dm^3$ $cm^{-1}$). $\Lambda_m$ (DMF, 298 K): 145 S $cm^2$ $mol^{-1}$.

**[TbCuL(DMF)](ClO$_4$)$_2$·MeCN 3.** Was synthesized by a method similar to **1**. Yield: 0.084 g, 66%. Found: C, 38.86; H, 3.72; N, 10.96; $C_{41}H_{46}Cl_5N_{10}O_{12}CuTb$ requires: C, 38.74; H, 3.65; N, 11.06%. IR (KBr, $cm^{-1}$): 1645s [$\nu$(C=N)]; 1541s [$\nu$(C–O)]; 1090s [$\nu(ClO_4)$]; 625m [$\nu(ClO_4)$]. [UV-Vis($\lambda_{max}$(nm), MeCN)]: 848 (60 $mol^{-1}$ $dm^3$ $cm^{-1}$), 506(shoulder), 378 (17400 $mol^{-1}$ $dm^3$ $cm^{-1}$), 245 (64200 $mol^{-1}$ $dm^3$ $cm^{-1}$), 227 (73300 $mol^{-1}$ $dm^3$ $cm^{-1}$). $\Lambda_m$ (DMF, 298 K): 145 S $cm^2$ $mol^{-1}$.

**[YCuL(DMF)](ClO$_4$)$_2$·MeCN 4.** Was synthesized by a method similar to **1**. Yield: 0.060 g, 50%. Found: C, 40.69; H, 3.92; N, 11.50; $C_{41}H_{46}Cl_5N_{10}O_{12}CuY$ requires: C, 40.99; H, 3.86; N, 11.71%. IR (KBr, $cm^{-1}$): 1645s [$\nu$(C=N)]; 1541s [$\nu$(C–O)]; 1090s [$\nu(ClO_4)$]; 625m [$\nu(ClO_4)$]. [UV-Vis($\lambda_{max}$(nm), MeCN)]: 850 (55 $mol^{-1}$ $dm^3$ $cm^{-1}$), 500(shoulder), 379 (17600 $mol^{-1}$ $dm^3$ $cm^{-1}$), 243 (68600 $mol^{-1}$ $dm^3$ $cm^{-1}$), 224 (80900 $mol^{-1}$ $dm^3$ $cm^{-1}$). $\Lambda_m$ (DMF, 298 K): 142 S $cm^2$ $mol^{-1}$.

**[DyCuL(DMF)](ClO$_4$)$_2$·MeCN 5.** Was synthesized by a method similar to **1**. Yield: 0.051 g, 40%. Found: C, 38.20; H, 3.75; N, 10.45; $C_{41}H_{46}Cl_5N_{10}O_{12}CuDy$ requires: C, 38.65; H, 3.64; N, 10.99%. IR (KBr, $cm^{-1}$): 1645s [$\nu$(C=N)]; 1541s [$\nu$(C–O)]; 1090s [$\nu(ClO_4)$]; 625m [$\nu(ClO_4)$]. [UV-Vis($\lambda_{max}$(nm), MeCN)]: 852 (60 $mol^{-1}$ $dm^3$ $cm^{-1}$), 496(shoulder), 381 (15600 $mol^{-1}$ $dm^3$ $cm^{-1}$), 244 (56000 $mol^{-1}$ $dm^3$ $cm^{-1}$), 225 (69000 $mol^{-1}$ $dm^3$ $cm^{-1}$). $\Lambda_m$(DMF, 298 K): 150 S $cm^2$ $mol^{-1}$.

### Physicochemical measurements

Elemental analyses were performed on a Perkin-Elmer 240c analytical instrument. The molar electrical conductivity of the complexes in DMF solution was measured on a BSD-A conductometer. The IR spectra were measured as KBr discs on a Nicolet 5 DX FT-IR spectrometer. Electronic spectra were recorded on a UV-3100 spectrophotometer. The electrospray mass spectra (ES-MS) were determined on a Finnigan LCQ mass spectrograph, the concentration of the samples were about 1.0 μmol $dm^{-3}$. The diluted solutions were electrosprayed at a flow rate of $5 \times 10^{-6}$ $dm^{-3}$ $min^{-1}$ with a needle voltage of +4.5 kV. The mobile phase was an aqueous solution of methanol (v/v, 1 : 1) and the samples was run in the positive-ion mode.

Variable-temperature magnetic susceptibility was measured on a SQUID-based sample magnetometer at an applied field of 5000 G over the temperature range 4–300 K. Diamagnetic corrections were made on the basis of Pascal constants ($-311 \times 10^{-6}$ emu $mol^{-1}$).[17]

The cyclic voltammetric experiments were performed on a PAR Model 273 potentiostat coupled to a PAR Model 175 universal programmer. A three-electrode system was used in all experiments. A glassy carbon electrode was employed as working electrode, an Ag–AgCl as reference electrode and a platinum coil wire as auxiliary electrode. Ferrocene was used as internal standard for the experiments. It has been proposed that the oxidation of ferrocene to ferrocenium ion occurs at the same potential in some solvents. In water the process occurs at +0.400 V *vs*. NHE or at +0.160 V *vs*. SCE.[18] Experiments were performed under a purified nitrogen atmosphere at 25 ± 0.1 °C. All the complex concentrations were $1.05 \times 10^{-3}$ mol $dm^{-3}$ in 0.1 mol $dm^{-3}$ TBAP (tetrabutylammonium perchlorate) DMF solutions. The solutions were deaerated for *ca.* 15 min before applying the voltage. The half wave potentials, $E_{1/2}$, were calculated approximately from $(E_{pa} + E_{pc})/2$ and the measured errors were ±2 mV. Unless otherwise stated, all potentials reported are referenced to NHE.

**Table 1** Crystallographic data for [EuCuL(DMF)](ClO$_4$)$_2$·MeCN

| | |
|---|---|
| Empirical formula | $C_{41}H_{46}Cl_5N_{10}O_{12}EuCu$ |
| Formula | 1263.63 |
| Crystal system | Monoclinic |
| Space group | $P2(1)/c$ |
| $T$/K | 293(2) |
| $a$/Å | 19.6888(12) |
| $b$/Å | 11.8254(6) |
| $c$/Å | 21.5616(12) |
| $\beta$/° | 98.6360(10) |
| $U$/Å$^3$, $Z$ | 4963.2(5), 4 |
| $\mu$(Mo-Kα)/$mm^{-1}$ | 2.019 |
| Reflections collected | 25135 |
| Independent reflections | 8772 [$R_{int}$ = 0.0884] |
| Goodness of fit on $F^2$ | 1.126 |
| Final $R1$, $wR2$ [$I > 2\sigma$] | 0.0709, 0.1254 |
| (all data) | 0.1407, 0.1538 |

### X-Ray crystal structure determination

Selected crystals of [EuCuL(DMF)](ClO$_4$)$_2$·MeCN were mounted on a SMART CCD diffractometer. Reflection data were measured at 293 K using graphite monochromated Mo-Kα ($\lambda$ = 0.71073 Å) radiation. The collected data were reduced using the program SAINT[19] and empirical absorption correction was done using the SADABS[20] program. The structure was solved by direct methods and refined by full-matrix least-squares methods on $F^2$ using the SHELXTL[21] software package. All the non-hydrogen atoms were anisotropically refined. The hydrogen atoms were geometrically fixed and allowed to ride on the parent atoms to which they were attached. The molecule graphics were created using SHELXTL. Atomic scattering factors and anomalous dispersion corrections were taken from the *International Tables for X-Ray Crystallography*.[22] Selected crystallographic data are collected in Table 1.

CCDC reference number 180262.

See http://www.rsc.org/suppdata/dt/b2/b201970a/ for crystallographic data in CIF or other electronic format.

## Results and discussion

### Synthesis and characterization

The cryptates [LnCuL(DMF)](ClO$_4$)$_2$·MeCN [Ln = Gd(III), Eu(III), Tb(III), Dy(III),Y(III)] were synthesized by a two-step process: (1) the mononuclear cryptate precursors, [Ln($H_3$L)-($NO_3$)($H_2O$)](ClO$_4$)$_2$,[23] were synthesized; (2) the heterodinuclear cryptates were formed by the reaction of the precursors with copper(II) ion. Because the Ln(III) ions in the cryptates are kinetically inert and thermodynamically stable while the encapsulated water molecule is labile, copper(II) ion replaced the water molecule during the reaction process. Added base removed the protons of the phenolic groups in the precursor. Due to the flexibility of the cryptand it was able to adjust its cavity to match the differently sized metal ions. Our synthesized method is different from that for Robson-type planar

**Table 2** The assignment of ES-MS peaks for $[LnCuL(DMF)](ClO_4)_2 \cdot MeCN$ (Ln = Gd, Eu, Tb, Dy,Y)

| Complex | Ln(III) | Peaks (*m/z*)[a] | Assignment |
|---|---|---|---|
| **1** | Gd(III)[b] | 1020.4 (18) | $[GdCuL(L - Cl) + ClO_4]^+$ |
| | | 996.7 (5) | $\{[GdCu(L - 3Cl) + MeOH + ClO_4^-]_2 + MeOH\}^{2+}$ |
| | | 514.3 (16) | $[GdCuL(DMF)]^{2+}$ |
| | | 494.0 (32) | $[GdCuL + MeOH]^{2+}$ |
| | | 478.2 (100) | $[GdCuL]^{2+}$ |
| **2** | Eu(III)[b] | 970.1 (10) | $[EuCuL + OH^-]^+$ |
| | | 861.2 (5) | $[EuCu(L - 3Cl) + OH^-]^+$ |
| | | 511.9 (10) | $[EuCuL(DMF)]^{2+}$ |
| | | 491.3 (50) | $[EuCuL + MeOH]^{2+}$ |
| | | 475.7 (100) | $[EuCuL]^{2+}$ |
| **3** | Tb(III)[c] | 1056.1 (18) | $[TbCuL + ClO_4^-]^+$ |
| | | 1016.1 (80) | $[TbCuL + MeCN + OH^-]^+$ |
| | | 991.3 (16) | $[TbCu(L - 3Cl) + ClO_4^- + MeCN]^+$ |
| | | 478.7 (100) | $[TbCuL]^{2+}$ |
| **4** | Y(III)[c] | 986.1 (8) | $[YCuL + ClO_4^-]^+$ |
| | | 946.1 (65) | $[YCuL + MeCN + OH^-]^+$ |
| | | 443.7 (100) | $[YCuL]^{2+}$ |
| **5** | Dy(III)[b] | 1080.1 (12) | $[DyCu(L - 3Cl) + ClO_4^- + MeCN + MeOH + 3H_2O]^+$ |
| | | 1067.1 (24) | $[DyCu(L - 3Cl)(DMF) + ClO_4^- + MeCN]^+$ |
| | | 1026.1 (42) | $[DyCu(L - 3Cl)(DMF) + ClO_4^-]^{2+}$ |
| | | 987.0 (32) | $[DyCu(L - 3Cl) + ClO_4^- + H_2O]^+$ |
| | | 484.1 (100) | $[DyCu(L - 3Cl)(DMF)(MeCN)]^{2+}$ |

[a] Relative abundances (%) are given in parentheses. [b] In methanol solution. [c] In acetonitrile solution.

macrocyclic heterodinuclear complexes. These Robson-type complexes were synthesized by (2 + 1) condensation of aldehyde with amine in the presence of metal ions and then by cyclization with another molecule of amine with the second metal ion acting as a template. The values of molar conductivity of the three complexes are located in the range of 1 : 2 electrolytes in DMF.[24] The IR spectrum of each complex showed an intense band at 1645 $cm^{-1}$ attributable to $\nu$(C=N) which was different from the split bands of the mononuclear cryptates due to the unsymmetrical coordination of lanthanide(III) ion to imino nitrogen atoms. The bands at 1090 and 625 $cm^{-1}$ are characteristic of $ClO_4^-$. The UV spectra of these cryptates are dominated by intense ligand bands at *ca.* 226, 245 and 378 nm, the band at 378 nm is assigned to the C=N chromophores, the other two bands are designated as a $\pi$–$\pi^*$ transition of the K band of the benzene rings. The d–d transition of Cu(II) in cryptates is at about 850 nm, showing that Cu(II) ions are located in an octahedral coordination environment.

### Electrospray mass spectra

The ES-MS data of cryptates are listed in Table 2. The most intense peak for each cryptate corresponds to the loss of a coordinated DMF molecule, forming fragments $[LnCuL]^{2+}$ which confirms the presence of Ln(III)–Cu(II) core in the cryptate. The other peak clusters of the fragments are assigned to binding of the $[LnCuL]^{2+}$ core with solvent molecules or $ClO_4^-$ as well as cryptand ligands losing three chlorine atoms from the phenyl rings. All the peaks displayed in the ES-MS spectra of the five cryptates can be assigned, confirming their good purity. Using the natural isotopic abundances of the atoms in $[GdCuL]^{2+}$, a revised program[25] was used to calculate the isotopic distribution at *m/z* = 478.2. The calculated pattern [Fig. 1(b)] is similar to the experimental one [Fig. 1(a)] and further confirms that the heterodinuclear complexes exist in solution.

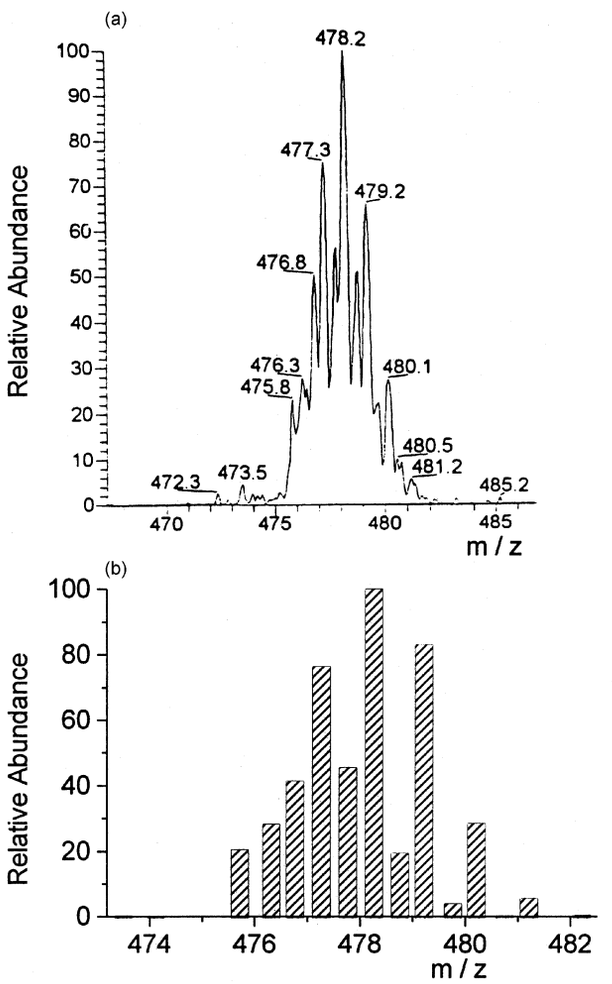


**Fig. 1** The isotopic pattern for $[GdCuL]^{2+}$ at *m/z* 478.2. (a) Observed isotopic distribution. (b) Calculated isotopic distribution.

### Crystal structure of $[EuCuL(DMF)](ClO_4)_2 \cdot MeCN$ 2

A summary of key crystallographic information is given in Table 1 and selected bond distances and angles are listed in Table 3. Structure analysis of cryptate **2** confirmed that the complex is a dinuclear Eu(III)–Cu(II) entity which is isostructural with Dy(III)–Cu(II) **5**.[14] The structure of complex cation $[EuCuL(DMF)]^{2+}$ is shown in Fig. 2. The Eu(III) ion is located at one end of the cavity and is eight-coordinated with the bridgehead nitrogen atom N(1), three imino-nitrogen atoms [N(2), N(3), N(4)], the oxygen atom O(4) of DMF and three phenoxy atoms [O(1), O(2), O(3)]. The coordination configuration is best described as distorted dodecahedral.

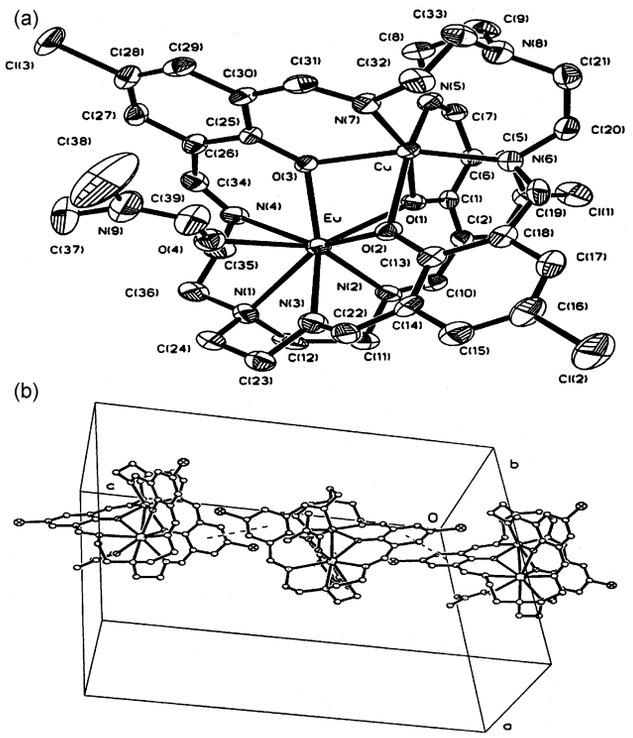


**Fig. 2** The crystal structure of $[EuCuL(DMF)]^{2+}$. (a) Perspective view. (b) Packing diagram.

The other end of the cavity was occupied by a Cu(II) ion, three μ-phenolate oxygen atoms and three imino-nitrogen atoms coordinated to Cu(II), forming a distorted octahedral configuration. A comparison of the structure data for some mono- and hetero-nuclear lanthanide cryptates is made in Table 4. (1) Comparing the bond lengths of mononuclear cryptates with heteronuclear crptates $[LnCuL(DMF)](ClO_4)_2$ (Ln = Eu, Dy, Y), it is seen that the coordination bond lengths of Ln–O(phenol), Ln–N(imino) and Ln–N(bridge) in heteronuclear cryptates are shorter than those in corresponding mononuclear cryptates which implies that an interaction exists between Ln(III) and Cu(II). (2) In both the mononuclear lanthanide and the heteronuclear cryptates, along with the decreasing radii of the lanthanide ions, not only the coordination bond lengths but also the distances between the two bridgehead nitrogen atoms decreased, *i.e.* the cavity radii of the cryptates decreased to match the smaller lanthanide ions. (3) In the heteronuclear cryptates, the bond distances Cu–O(phenol) also decreased along with the decreasing radii of the lanthanide ions. Little regularity was found for the Cu–N(imino) lengths, implying that the interaction of Ln(III) with Cu(II) ions involves phenoxy atoms. The above mentioned facts indicate that the cryptands are able to adjust the size of their cavities to suit the requirements of the coordination configuration.

**Table 3** Selected bond distances (Å) and angles (°) for $[EuCuL(DMF)](ClO_4)_2$·MeCN

| | | | |
|---|---|---|---|
| Eu–O(1) | 2.345(6) | Eu–N(4) | 2.490(8) |
| Eu–O(2) | 2.283(6) | Cu–O(1) | 2.192(6) |
| Eu–O(3) | 2.342(6) | Cu–O(2) | 2.404(6) |
| Eu–O(4) | 2.400(8) | Cu–O(3) | 2.023(6) |
| Eu–N(1) | 2.639(8) | Cu–N(5) | 2.194(8) |
| Eu–N(2) | 2.489(8) | Cu–N(6) | 1.991(8) |
| Eu–N(3) | 2.519(8) | Cu–N(7) | 2.031(8) |
| Cu–O(1)–Eu | 92.1(2) | Cu–O(3)–Eu | 96.7(2) |
| Cu–O(2)–Eu | 88.4(2) | | |

In cryptate **2**, the angle between the benzene ring ($C_{13}$–$C_{18}$) (symmetry: $x$, $y$, $z$) of one molecule and that ($C_{25}$–$C_{30}$) (symmetry: $x$, $0.5 - y$, $-0.5 + z$) of the neighbouring molecule is 13.7°. The distance between the planes of two neighbouring benzene rings is about 3.44 Å which indicates that cryptate molecules are arranged into a one-dimensional chain along the $c$-axis and by π–π stacking [Fig. 2(b)]. The intermolecular π–π stack also exists in other heteronuclear cryptates. In heterodinuclear cryptates, the angles between benzene rings of neighbouring molecules increased along with the lanthanide ion radii. These regularities for Ln–Cu cryptates are also suitable for Ln–Ni cryptates which will be reported elsewhere.

### Magnetic properties of $[GdCuL(DMF)](ClO_4)_2$·MeCN

The temperature ($T$) dependence of magnetic susceptibility ($\chi_m$) in the range 3.50–300 K is shown in Fig. 3. The effective magnetic moment $\mu_{eff}$ at 300.17 K is 8.03 $\mu_B$ which is slightly lower than the spin-only value (8.12 $\mu_B$) calculated by $\mu_{eff}^2 = \mu_{Cu}^2 + \mu_{Gd}^2$ by assuming that there is no magnetic interaction between Cu(II) ($S_{Cu}$ = 1/2) and Gd(III) ($S_{Gd}$ = 7/2). As the temperature was lowered, the $\mu_{eff}$ increased slowly from 8.04 $\mu_B$ at 300.17 K to 8.10 $\mu_B$ at 50 K and then increased steeply to the maximum value (8.50 $\mu_B$) at 3.50 K. The maximum value is smaller than the spin-only value (8.94 $\mu_B$) for spin state $S$ = 4

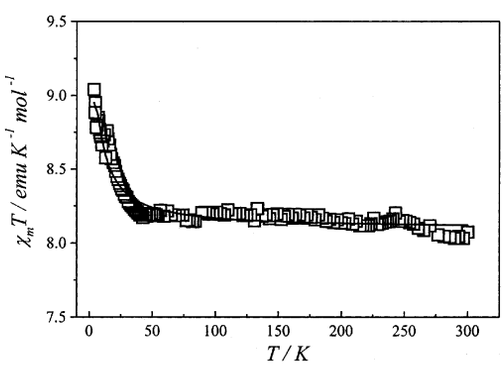


**Fig. 3** A plot of $\chi_m T$ *vs.* $T$ for $[GdCuL(DMF)](ClO_4)_2$·MeCN. Squares: experimental data; full line: fitting curve.

**Table 4** Comparison of bond lengths (Å) and angles (°) between lanthanide mononuclear $[Ln(H_3L)(NO_3)(H_2O)](ClO_4)_2$ and heteronuclear cryptates $[LnCuL(DMF)](ClO_4)_2$·MeCN (Ln = Eu, Dy, Y)

| Average values | Eu[a] | Eu–Cu | Dy[d] | Dy–Cu[b] | Y[c] | Y–Cu[d] |
|---|---|---|---|---|---|---|
| Ln–O(phenol) | 2.360 | 2.323 | 2.325 | 2.299 | 2.317 | 2.174 |
| Ln–O($NO_3^-$ or DMF) | 2.570 | 2.400 | 2.559 | 2.340 | 2.456 | 2.172 |
| Ln–N(imino) | 2.527 | 2.499 | 2.509 | 2.475 | 2.489 | 2.459 |
| Ln–N(bridge) | 2.761 | 2.639 | 2.701 | 2.617 | 2.674 | 2.601 |
| N–N(bridge) | 8.407 | 9.050 | 8.307 | 9.003 | 8.239 | 8.999 |
| Cu–O(phenol) | | 2.206 | | 2.187 | | 2.175 |
| Cu–N(imino) | | 2.072 | | 2.081 | | 2.082 |
| Ln–Cu | | 3.269 | | 3.225 | | 3.247 |
| Ln–O–Cu | | 92.4 | | 93.1 | | 93.1 |
| Angles between two benzene rings | | 13.7 | | 12.9 | | 12 |

[a] Ref. 11*d*. [b] Ref. 14*a*. [c] Ref. 23*c*. [d] Q.-Y. Chen, PhD. Thesis, Nanjing University, May 2001.

which arises from ferromagnetic spin-coupling of the present spin system ($S_{Cu}$ = 1/2, $S_{Gd}$ = 7/2). Therefore the observed magnetic behaviour clearly demonstrates an intramolecular ferromagnetic spin-coupling between Cu(II) and Gd(III) and, possibly, an intermolecular antiferromagnetic coupling interaction in the cryptate. The magnetic data were analyzed on the base of the spin-only equation derived from a spin Hamiltonian $H = -JS_{Cu}S_{Gd}$, $\chi_m$ is expressed as follows:

$$\chi_m = \frac{4Ng^2\beta^2}{kT}\left[\frac{15 + 7\exp(-8J/kT)}{9 + 7\exp(-8J/kT)}\right] \quad (1)$$

On fitting eqn. (1), the parameters $g$ = 1.99 and $J$ = +0.68 $cm^{-1}$ were obtained with an agreement factor $R = 6.30 \times 10^{-4}$ [$R = \Sigma(\chi_{obs}T - \chi_{calc}T)^2/\Sigma(\chi_{obs}T)^2$; $\chi_{calc}$ and $\chi_{obs}$ denote the calculated and observed molar magnetic susceptibilities, respectively]. The positive $J$ value is in agreement with the intramolecular ferromagnetic interaction. The analogous Schiff-base complexes with $CuO_2Gd$-type bridging networks and two identical oxygen donors afforded by phenolic groups have been reported previously.[9,26] The interaction between Gd(III) and Cu(II) ions could be either ferromagnetic or antiferromagnetic,[27] their $J$ constants vary from −0.49 to + 10.1 $cm^{-1}$.[9] The cryptate **1** whose Gd(III) and Cu(II) ions are bridged by three μ-oxygen atoms of phenolic groups displays a weak intramolecular ferromagnetic interaction. The ferromagnetic contribution resulted from the interaction of the ground-state configuration with the first excited charge-transfer configuration in which an unpaired electron of Cu(II) was transferred into the empty 5d orbital of Gd(III) according to a mechanism suggested by Goodenough.[28]

### Cyclic voltammetric behaviour

While scanning from 0 to −1.8 V with a potential scan rate of 0.05 V $s^{-1}$, the mononuclear cryptates $[Dy(H_3L)(NO_3)(H_2O)](ClO_4)_2$ did not display any peaks in DMF solution. The cyclic voltammogram of cryptate **5** is shown in Fig. 4. One pair

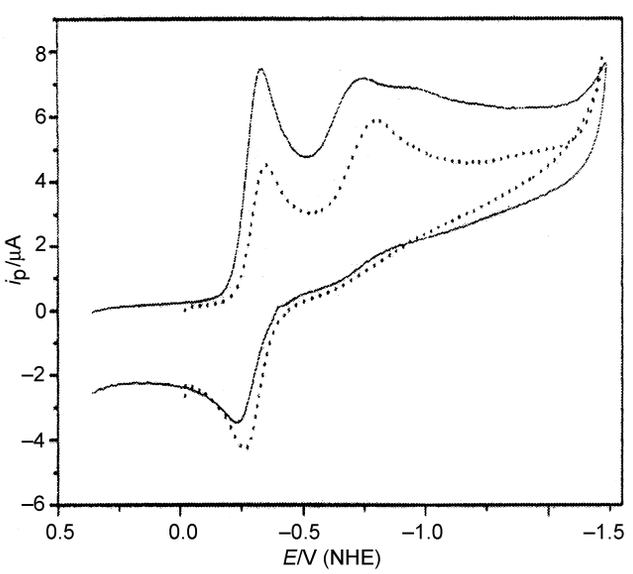


**Fig. 4** Cyclic voltammograms of $[LnCuL(DMF)](ClO_4)_2 \cdot MeCN$ (Ln = Eu, full line; Dy, dashed line) in DMF solutions. [Complex] = $1.05 \times 10^{-3}$ mol $dm^{-3}$, [TABP] = 0.1 mol $dm^{-3}$, scan rate = 0.050 V $s^{-1}$.

of well-defined cathodic and anodic peaks with peak potentials $E_{pc}^1$ = −0.263 V, $E_{pa}^1$ = −0.327 V (*vs.* NHE) was observed and the half-wave potential $E_{1/2}$ was calculated to be −0.295 V (*vs.* NHE). The peak potential separation $\Delta E^1$ was 66 mV and increased with increasing scan rate. The ratios of anodic to cathodic peak currents $i_{pc}/i_{pa}$ were close to unity at low scan rates. The plot of $i_{pc}^1$ (or $i_{pa}^1$) against the square root of potential scan rate $v^{1/2}$ was a straight line which indicates that the electrode process can be characterized as a quasi-reversible $Dy^{III}Cu^{II}/Dy^{III}Cu^{I}$ redox process. In addition, another cathodic peak with peak potentials $E_{pc}^2$ = −0.770 V was also presented, corresponding to the irreversible $Dy^{III}Cu^{I}/Dy^{III}Cu^{0}$ redox process, its anodic peak was poorly defined, so that its value of peak potential can not be obtained accurately. Except the above mentioned two pairs of peaks, no other peaks were found in the cyclic voltammogram, implying that Dy(III) was not reduced or oxidized. The overall electrode reaction of cryptate **5** can be presented as follows:

$$[Dy^{III}Cu^{II}L]^{2+} \xrightarrow{e} [Dy^{III}Cu^{I}L]^{+} \xrightarrow{e} [Dy^{III}Cu^{0}L] \quad (2)$$

Scanning from +0.2 to −0.7 V, the cyclic voltammogram of $[EuCuL(DMF)](ClO_4)_2 \cdot MeCN$ **2** showed well-defined cathodic and anodic peaks with peak potentials $E_{pc}^1$ = −0.308 V, $E_{pa}^1$ = −0.228 V. The half-wave potential $E_{1/2}$ was calculated to be −0.268 V (*vs.* NHE), which is close to the redox potential value of $Dy^{III}Cu^{II}/Dy^{III}Cu^{I}$ in cryptate **5**, corresponding to the $Eu^{III}Cu^{II}/Eu^{III}Cu^{I}$ redox process. When scanning continuously to −1.8 V, in addition to the pair of peaks mentioned above, two irreversible broad peaks were also observed (Fig. 4). Comparing the redox process of **2** with that of cryptate **5**, the more positive peak with $E_{pc}^2$ = −0.720 V was attributed to the irreversible $Eu^{III}Cu^{I}/Eu^{III}Cu^{0}$ redox process. Because the mononuclear cryptate $[Eu(H_3L)(NO_3)(H_2O)](ClO_4)_2$ with the same ligand has the potential values $E_{pc}$ = −0.860 V, $E_{pa}$ = −0.780 V and $E_{1/2}$ = −0.820V, the more negative weak peak with $E_{pc}^3$ = −0.964 V (*vs.* NHE) should be attributed to the irreversible $Eu^{III}Cu^{0}/Eu^{II}Cu^{0}$ process. The weak peak was partly overlapped with the reduction peak of copper(I).

The cryptates **1**, **3** and **4** have similar voltammetric properties to **5**, each cryptate showing a pair of well-defined redox peaks and an irreversible cathodic peak corresponding to stepwise reduction of the copper(II) ion. The electrochemical data for cryptates **1**–**5** are listed in Table 5. From Table 5 we can see that the $E_{1/2}^1$ values of copper(II) ions shift negatively compared with free $Cu^{2+}$ and are influenced by the lanthanide(III) ion encapsulated in the cryptate. The sequence of influence for Ln ions is: Dy > Tb ⩾ Gd > Eu. The higher the f-electron number of the lanthanide(III) ion, the more negative the $E_{1/2}^1$ values are and the more difficult it is to reduce copper(II) in the cryptates. This is in agreement with the sequences of decreasing bond lengths for Cu–O(phenol) and Ln–O(phenol) obtained by single crystal X-ray analyses.

**Table 5** The potential values (V, *vs.* NHE) of $[LnCuL(DMF)](ClO_4)_2 \cdot MeCN$ (Ln = Gd, Eu, Tb, Dy, Y) cryptates in DMF, scan rate 0.020 V $s^{-1}$

| Ln | $-E_{pc}^1$/V | $-E_{pa}^1$/V | $-E_{1/2}^1$/V | $-E_{pc}^2$/V | $-E^3{}_{Pc}$/V |
|---|---|---|---|---|---|
| Eu | 0.308 | 0.228 | 0.268 | 0.720 | 0.964 |
| Gd | 0.306 | 0.238 | 0.272 | 0.724 | |
| Tb | 0.322 | 0.258 | 0.290 | 0.760 | |
| Dy | 0.327 | 0.263 | 0.295 | 0.770 | |
| Y | 0.304 | 0.229 | 0.267 | 0.812 | |

The measured errors were ±2 mV.

## Conclusion

Five heterodinuclear cryptates $[LnCuL(DMF)](ClO_4)_2 \cdot MeCN$ (Ln = Gd, Eu, Tb, Dy, Y) were synthesized by a two-step method. The ES-MS spectra showed that the complexes are strict dinuclear entities and that the Ln(III)–Cu(II) cores are very stable in solution. Comparison of crystalline structure data for the heteronuclear cryptates showed that the coordination bond lengths of Ln(III) ions and Cu–O(phenol) decreased with

decreasing radii of the Ln(III) ions. The cyclic voltammogram of each cryptate showed a pair of well-defined redox peaks and an irreversible cathodic peak assigned to the stepwise reduction of Cu(II). The $E_{1/2}$[1] values of Cu(II) ions shifted negatively compared to free $Cu^{2+}$ ion and was influenced by lanthanide ions in the cryptates. The degree of negative-shift follows the order: Dy > Tb ⩾ Gd > Eu. Variable temperature magnetic susceptibility confirms the existence of a weak intramolecular ferromagnetic interaction in the Gd(III)–Cu(II) cryptate.

## Acknowledgements

This project was supported by the National Science Foundation of China, Foundation of Fuzhou, State Key Laboratory of Structure Chemistry and the Foundation of the State Key Laboratory of Lanthanide and Materials Chemistry of Beijing University.

## References

1 (*a*) P. Zanello, S. Tamburini, P. A. Vigato and G. A. Mazzocchin, *Coord. Chem. Rev.*, 1987, **77**, 165; (*b*) B. Bosnich, *Inorg. Chem.*, 1999, **38**, 2554; (*c*) J.-P. Costes, A. Dupuis and J.-P. Laurent, *J. Chem. Soc., Dalton Trans.*, 1998, 735.
2 (*a*) J.-L. Pierre, *Chem. Soc. Rev.*, 2000, **29**, 229; (*b*) L. Que, Jr. and Y. N. Ho Raymend, *Chem. Rev.*, 1996, **96**, 2607; (*c*) M. Shinoura, S. Kita, M. Ohba, H. Okawa, H. Furutachi and M. Suzuki, *Inorg. Chem.*, 2000, **39**, 4520; (*d*) Q. Lu, Q.-H. Luo, A. B. Dai, Z. Zhou and G.-Z. Hu, *J. Chem. Soc., Chem. Commun.*, 1990, **5**, 1429.
3 (*a*) R. Blunt, *Chem. Ber.*, 1983, **19**, 740; (*b*) A. Poddar, P. Mandal, P. Choudhury, A. N. Das. and B. Ghosh., *J. Phys. Chem.*, 1988, **21**, 3323; (*c*) E. P. Boyd, D. R. Ketchum, H. Deng and S. G. Shore, *Chem. Mater.*, 1997, **9**, 1154.
4 D. W. Knoeppel, J. Liu, E. A. Meyers and S. G. Shore, *Inorg. Chem.*, 1998, **37**, 4828.
5 (*a*) D. Parker and J. A. G. Williams, *J. Chem. Soc., Dalton Trans.*, 1996, 3613; (*b*) F. Richardson, *Chem. Rev.*, 1982, **82**, 541; (*c*) G. Mathis, *Clin Chem. (Washington, D. C.)*, 1993, **39**, 1953; (*d*) E. Soini and I. Hemmila, *Clin. Chem.*, 1979, **25**, 353.
6 (*a*) C. H. Evans, *Biochemistry of Lanthanide*, Plenum, New York, 1990; (*b*) P. Caraven, J. J. Ellison, T. J. McMurry and R. B. Lauffer, *Chem. Rev.*, 1999, **99**, 2293.
7 J. R. Morrow, K. A. Kolasa, S. Amin and K. O. A. Chin, *Adv. Chem. Ser.*, 1995, **246**, 431.
8 (*a*) Z.-Q. Xu, P. W. Pead, D. E. Hibbs, M. B. Hursthouse, K. M. A. Malik, B. O. Retting, M. Seid, D. A. Summers, M. Pink, R. C. Thompson and C. Orvig, *Inorg. Chem.*, 2000, **39**, 508; (*b*) J.-P. Costes, F. Dahan, A. Dupuis and J.-P. Laurent, *Inorg. Chem.*, 1997, **36**, 3429; (*c*) E. K. Brechin, S. G. Harris, S. Parsons and P. E. P. Winpenny, *J. Chem. Soc., Dalton Trans.*, 1997, 1665.
9 (*a*) J.-P. Costes, F. Dahan and A. Dupuis, *Inorg. Chem.*, 2000, **39**, 165; (*b*) I. Ramade, O. Kahn, Y. Jeanin and F. Robert, *Inorg. Chem.*, 1997, **36**, 930; (*c*) C. Piguet, C. Edder, S. Rigault, G. Bernardinelli, J.-C. G. Bunzli and G. Hopfgartner, *J. Chem. Soc., Dalton Trans.*, 2000, 3999.
10 (*a*) B. Alpha, J.-M. Lehn and G. Mathis, *Angew. Chem., Int. Ed. Engl.*, 1987, **26**, 266; (*b*) N. Sabbatini and M. Guardigli, *Coord. Rev.*, 1993, **123**, 201.
11 (*a*) C. Platas, F. Avecilla, A. de Blas, T. Rodrigues-Blas, C. F. G. C. Geraldes, E. Toth, A. E. Merbach and J.-C. G. Bunzli, *J. Chem. Soc., Dalton Trans.*, 2000, 611; (*b*) C. Platas, C. F. G. C. Geraldes, T. Rodriguez-Blas, H. Adams and J. Mahia, *Inorg. Chem.*, 1999, **38**, 3190; (*c*) F. Avecilla, R. Bastida, A. de Blas, D. E. Fenton, A. Macias, A. Rodriguez, T. Rodriguez-Blas, S. Garcia-Granda and R. Corza-Suarez, *J. Chem. Soc., Dalton Trans.*, 1997, 409; (*d*) Q.-Y. Chen, C.-J. Feng, Q.-H. Luo, C.-Y. Duan, X.-S. Yu and D.-J. Liu, *Eur. J. Inorg. Chem.*, 2001, 1067.
12 M. G. B. Drew, O. W. Howarth, C. J. Harding, N. Martin and J. Nelson, *J. Chem. Soc., Chem. Commun.*, 1995, 903.
13 F. Avecilla, A. De Bias, R. Bastida, D. E. Fenton, J. Mahia, A. Macias, C. Plates, A. Rodriguez and T. Rodriguez-Blas, *Chem. Commun.*, 1999, 125.
14 (*a*) Q.-Y. Chen, Q.-H. Luo, Z.-L. Wang and J.-T. Chen, *Chem. Commun.*, 2000, 1033; (*b*) Q.-Y. Chen, Q.-H. Luo, L.-M. Zheng, Z.-L. Wang and J.-T. Chen, *Inorg. Chem.*, 2002, **41**, 605.
15 S. Taniguchi, *Bull. Chem. Soc. Jpn.*, 1984, **57**, 2687.
16 E. Kimura, S. Young and J. P. Collman, *Inorg. Chem.*, 1970, **9**, 118.
17 *Progress in Inorganic Chemistry*, C. J. Connor and S. J. Lippard, eds., Wiley, New York, 1982, vol. 29, p. 203.
18 R. R. Gagne, C. A. Koval and G. C. Lisensky, *Inorg. Chem.*, 1980, **19**, 2855.
19 G. M. Sheldrick, SAINT (version 4), Siemens Analytical X-Ray Systems, Inc., Madison, Wisconsin, USA, 1994.
20 G. M. Sheldrick, SADABS, Absorption Correction Progam, University of Göttingen, Germany, 1996.
21 G. M. Sheldrick, SHELXTL (version 5.0), Siemens Analytical X-Ray systems, Inc., Madison, Wisconsin, USA, 1997.
22 A. J. Wilson, *International Tables for X-Ray Crystallography*, Kluwer Academic Publishers, Dordrecht, 1992, vol. C, Tables 6.1.1.4 and 4.2.6.8.
23 (*a*) C.-J. Feng, Q.-H. Luo, C.-Y. Duan, M.-C. Shen and Y.-J. Liu, *J. Chem. Soc., Dalton Trans.*, 1998, 1377; (*b*) Q.-Y. Chen, Q.-H. Luo, Y.-J. Liu and C.-Y. Duan, *J. Chem. Crystallogr.*, 2000, **30**, 177; (*c*) C.-J. Feng, Q.-H. Luo and Y.-Z. Xu, *Synth. React. Inorg. Met.-Org. Chem.*, 2000, **30**, 1449.
24 W. J. Geary, *Coord. Chem. Rev.*, 1971, **7**, 81.
25 J. D. Lee, *Talanta*, 1973, **20**, 1029.
26 (*a*) M. Sasaki, K. Manseki, H. Horiuchi, M. Kumagai, M. Sakamoto, H. Sakiyama, Y. Nishida, M. Sakai, Y. Sadaoka, M. Ohba and H. Okawa, *J. Chem. Soc., Dalton Trans.*, 2000, 259; (*b*) J.-P. Costes, F. Dahan, A. Dupuls and J.-P. Laurent, *Inorg. Chem.*, 1996, **35**, 2400.
27 J.-P. Costes, F. Dahan, A. Dupuis and J.-P. Laurent, *Inorg. Chem.*, 2000, **39**, 169.
28 J. B. Goodenough, *Magnetism and Chemical Bonding*, Interscience, New York, 1963.